Preprints.org

Article

Mossbauer Spectroscopy Investigation of Thulium Oxide-Hematite Magnetic Ceramic Nanostructures

Elena Stipetich , Sarah Glasser , Monica Sorescu [*]

Article

Mössbauer Spectroscopy Investigation of Thulium Oxide-Hematite Magnetic Ceramic Nanoparticles

Elena Stipetich, Sarah Glasser and Monica Sorescu *

Duquesne University, Department of Physics, Fisher Hall, Pittsburgh, PA 15282, USA

* Correspondence: sorescu@duq.edu; Tel.: +(412)-396-4166; Fax: (412)-396-4829

Abstract: Magnetic ceramic nanoparticles system xTm_2O_3-$(1-x)\alpha$-Fe_2O_3 (x=0.1 and 0.5) was synthesized by mechanochemical activation starting from hematite and thulium oxide precursors and characterized by transmission Mössbauer spectroscopy. The Mössbauer spectra were typically analyzed considering 1-3 sextets, corresponding to hematite (with and without thulium doping) and a doublet, representing thulium iron perovskite (thulium orthoferrite). The magnetic hyperfine fields (BHF) and doublet abundance were studied as function of the ball milling time (BMT) for both molar concentrations employed. The results are consistent with the formation of solid solutions in the investigated system. The mixed-oxide nanoparticle system synthesized may have important applications in displays, sensors and photovoltaics, and is paving the way for emerging utilizations related to mechanically flexible electronics.

Keywords: magnetic materials; nanocomposites; Mössbauer spectroscopy

1. Introduction

Many branches of today's economies rely on applications of thulium oxide (Tm_2O_3) [1–14]. Thulium oxide represents the next generation of neutron absorbers [1,2] and Tm_2O_3 thin films are developed as passive saturable absorbers for pulsed fiber laser generation [12]. Vitamin C detection of nanostructured Tm_2O_3 leads to applications in electrochemistry and bioelectronics [8]. Zirconia-doped thulium oxide (ZrO_2:Tm_2O_3) is highly transparent [5] and thulium vanadate-hematite nanocomposites ($TmVO_4$/Fe_2O_3) were demonstrated to show higher catalytic activity than the separate pure nanoparticles [7].

In order to obtain high resolution information on its properties, thulium oxide must be functionalized with an iron oxide, such as hematite (α-Fe_2O_3). Hematite has various applications in scientific and industrial fields and can be used as a semiconductor compound, magnetic material, catalyst and gas sensor. In this study we propose to synthesize the mixed oxide system xTm_2O_3-$(1-x)\alpha$-Fe_2O_3 at two molar concentrations (x=0.1 and 0.5) and characterize its structural and magnetic properties by ^{57}Fe Mössbauer spectroscopy. A similar approach was used recently for the characterization of other related rare earths oxides-hematite nanocomposites [15,16]. Semiconducting oxides have formed the basis for technological significant advancements in displays, sensors and photovoltaics, and are setting the stage for emerging applications related to mechanically flexible electronics.

High resolving power is the factor of Mössbauer spectroscopy which distinguishes it from other forms of spectroscopy. The Mössbauer Effect is the physical phenomenon of nuclei which absorb, emit, or scatter gamma photons with no recoiling. Since spectral lines of recoil free transitions are minuscule compared to interactions between nuclei and electrons, the recorded Mössbauer spectra have a hyperfine structure. It is this hyperfine structure which allows for such a high resolving power [17]. We currently aim to use this effect to reveal magnetic and structural information about different compounds using Mössbauer spectroscopy on hematite doped samples.

The hematite samples discussed in this paper were doped with two different concentrations of thulium oxide (x=0.1 and x=0.5). The purpose of this is to analyze the spectral lines of hematite and how they evolve as the entire sample of thulium oxide-hematite becomes mechanochemically

activated, gradually substituting thulium into the hematite lattice and affecting the overall hyperfine magnetic field. This evolution reveals the desired chemical and physical information about thulium oxide, which is very helpful for predicting and understanding the behavior of the compound. Thulium oxide is a rare earth metal oxide (rare earth metals are metals which occur in low abundance at Earth's surface—hence the name rare, but high abundance in the crust of the earth) with the chemical formula Tm_2O_3. One study [6] found that rare earth metal oxides have uses including but not limited to: photovoltaic cells for synthesis of solar energy, data storage and processing in MOS (metal oxide semiconductor) devices due to their high dielectric constant, batteries, hybrid vehicles, flat screen technology, agriculture (mostly in fertilizers), trace gas sensors and even medicine. Thulium oxide in particular has many uses especially in the areas of optics, electrochemistry and even bioelectronics. It has been shown to be an efficient passive saturable absorber in pulsed fiber lasers, as in the 1.55 micro-meter region it effectively generated laser pulsing of an erbium doped fiber laser when inserted into the ring cavity [12]. One experiment [8] successfully used thulium oxide to determine the amount of ascorbic acid (vitamin C) in an aqueous solution through irreversible oxidation of the ascorbic acid and analyzing the current of the sample across an electrode. This experiment truly emphasizes the possible uses of thulium oxide in the pharmaceutical/medical industries. Another study which examined the electrochemical behavior of thulium showed that thulium was easily reduced on aluminum electrodes, forming different alloy combinations between the two elements, which hints at an easy route for extraction of the rare earth metal from molten chlorides (somewhat promising for a rare earth metal for which a barrier for common usage is extraction) [18].

Due to its many uses in different areas of science and technology, it is important to understand the fundamental properties of thulium oxide to better predict its behavior, which is the purpose of this paper. However, there is already some existing information on the chemical properties. One study [19] found the distances between neighboring lattice planes of Tm_2O_3 to be 0.31 nm for planes with the Miller index (222) and 0.26 nm for planes with the Miller index (400). This same study also found that annealing (heating to decrease hardness and increase ductility) at 600° C produced no significant change in the lattice. Later in this study, the presence of thulium oxide in a carbon monoxide oxidation reaction was observed along with the energy level of the reaction. It was speculated that thulium oxide decreased the energy of oxidation for carbon monoxide, suggesting potential use as an oxidation reaction catalyst.

One can also look at the behavior of thulium itself to gain a better understanding of thulium oxide. One study [20] examined the behavior of different elements inside fullerenes (a spherical cage-like molecule of carbon), including thulium. One of these cage-like molecules with other atoms enclosed within its sphere is called an endohedral fullerene. Two thulium endohedral fullerene peaks on a mass spectrometry graph had too small of a distance to be examined without a form of high-resolution spectrometry due to its high atomic weight- emphasizing the importance of a high-resolution technique such as Mössbauer spectroscopy as applied to thulium oxide. Two articles about thulium molecules [21,22] might give important information about the magnetization of thulium ions. The first of these attempted to discern structural information about the isotope of thulium, [169]Tm through Mössbauer spectroscopy on the molecule Tm_2BaNiO_5 (which is antiferromagnetic due to the presence of nickel) by pelletizing, grinding and heating a mixture of Tm_2O_3, NiO and $BaCO_3$ in three different phases to achieve their desired "*Immm*" phase (*Immm* refers to a specific lattice symmetry which makes this molecule appear green). In each sample however, there was a leftover impurity of Tm_2O_3 present which appeared on the spectral graphs as a doublet with a large quadrupole splitting value- something which is discussed in the analysis section of this paper as well. Another useful piece of information we can extract from this study is their conjecture that the saturation point of the magnetic moment at the site of the thulium ions in their sample was exceptionally small, suggesting that the exchange interaction (a magnetic interaction where an atom attempts to align the magnetic moments of the surrounding atoms) between two thulium ions is negligible. In support of this, the latter aforementioned study (which followed a similar method of preparation and analysis as the

former for the molecule Tm_2BaCuO_5 which appears antiferromagnetic at high temperatures) also found that there was no independent magnetic ordering by the Tm^{3+} ions [22].

Even in light of the existing structural and behavioral information about thulium oxide, the present study on the Mössbauer spectra of thulium oxide doped hematite particles may still clarify much about the magnetic and nuclear properties of thulium. Already several studies have been performed in our solid state laboratory at Duquesne University which have demonstrated these properties in other rare earth metals such as ruthenium, iridium and europium [23]. Each of these studies used other methods to analyze the ball milled solids in addition to Mössbauer spectroscopy such as differential scanning calorimetry, thermal gravimetric analysis and/or x-ray powder diffraction to evaluate the properties of the systems in question. However, in each case Mössbauer spectroscopy played a crucial role in the observation of the hyperfine aspects of the compounds which other methods of analysis fall short of determining due to the limitations of lower resolving power. In all three cases with the increase of ball milling time, the Mössbauer spectroscopy showed evidence of the substitution of the rare earth metal into the hematite lattice giving rise to a nonmagnetic phase. This was determined with a decrease in hyperfine magnetic field in all cases and increase in percent abundance of the quadrupole split doublet on the graph in the ruthenium and europium samples due to the formation of perovskite compounds.

Our purpose in this study is to use the Mössbauer spectroscopy technique to examine the structural, chemical and magnetic properties of thulium oxide through spectral analysis of hematite doped with thulium oxide. In the following we will examine the methods, machines and software used to complete these tasks as well as the conclusive results.

2. Results and Discussion

The exchange interactions and nuclei-electron interactions fall into the category of hyperfine interactions. These hyperfine interactions are observed in this paper via gamma photon resonance observation, which is Mössbauer spectroscopy. It will be useful before describing the methodologies used in this project to examine the specifics of Mössbauer spectroscopy parameters.

The three important Mössbauer spectroscopy parameters we will cover are isomer shift, quadrupole splitting and the hyperfine magnetic field. Analysis of all three of these parameters is very important for interpreting the hyperfine structure of the Mössbauer spectra. It is also important to remember that the unique hyperfine structure created by the Mössbauer effect is only effective when used on atoms with specific energy levels that allow recoil free transitions to be much smaller than nuclei-electron interactions. ^{57}Fe is an example of one of these atoms, which is why hematite is commonly used for this specific type of spectroscopy [17].

The isomer shift of a Mössbauer spectrum (Figure 1) is due to the possibility of an s-electron occupying space inside the nucleus. S-electrons are the only electrons which are capable of doing so, and therefore are the sole, direct contribution to the isomer shift. When this happens, there is a small change in the nuclear energy level of the atom which is observable in our spectra as an electrostatic shift from the energy of the gamma ray source and the energy of the absorber. Graphically, this manifests itself as a horizontal shifting of the resonance line from zero velocity [17].
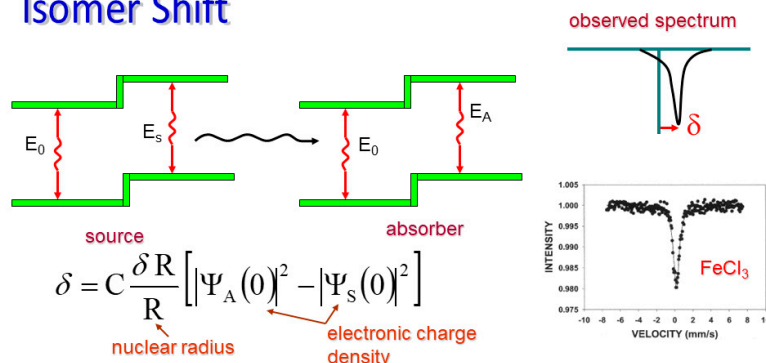
Figure 1. Isomer shift parameter.

The quadrupole splitting (Figure 2) of our spectra is extremely important, particularly in determination of different crystallographic inequivalent sites. It also reveals information about electronic structure, bond properties and molecular geometry of the analyzed material. The effect of quadrupole splitting is due to an interaction between the electric field gradient and the quadrupole moment of the nucleus. This interaction shifts the sublevels of the excited states by splitting the nuclear energy levels in two. Both of these new levels may have gamma transitions. The duality of the new upper levels translates into two resonances (peaks) on the spectral graph, where the distance between them is exactly equal to the change in energy of the split [17].
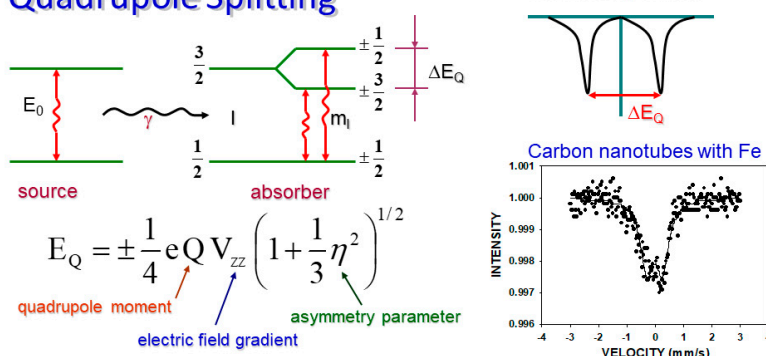

Figure 2. Quadrupole splitting parameter.

The last of our parameters, the magnetic hyperfine field, is essentially the net magnetic field at the nucleus (Figure 3). Specifically, it is the product of the nucleus's dipole moment interaction with the magnetic field at the nuclear site. In the case of ^{57}Fe (part of our hematite sample), this interaction allows six transitions creating a sextet on our spectral graph. This happens because the Zeeman effect dictates that this net magnetic field must split our nuclear energy levels. Specifically, our magnetic

field will degenerate the atomic energy levels into (2I + 1) sublevels where I corresponds to the spin of the state.
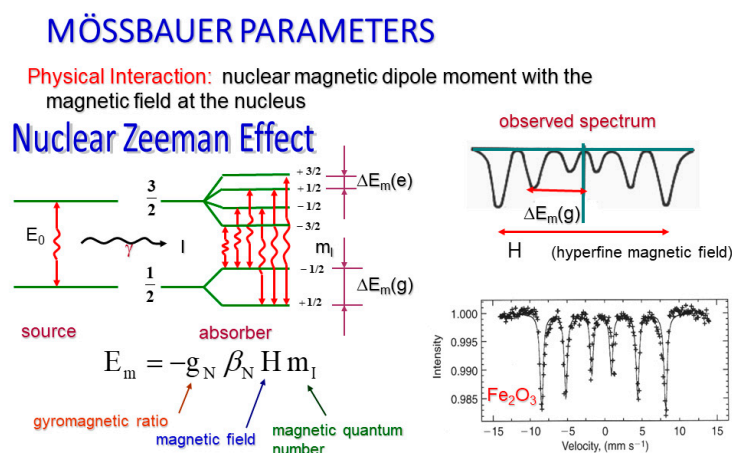
Figure 3. Hyperfine magnetic splitting parameter.

We also know that ^{57}Fe has its ground state where I=1/2 and its excited state where I=3/2, yielding six sublevels, which allows for our six gamma transitions and therefore a sextet of our recorded spectra, subject to magnetic dipole selection rules [17].

All together these parameters must be analyzed for a spectral graph to determine what information the graph holds. Each parameter contributes to each peak creating a very complicated overlap of influence which is best analyzed using least squares fitting of the Lorentzian line shapes (a curve with an inversely squared relationship to the horizontal variable). Using this method to estimate the best fitting parameters of the Mössbauer spectroscopy performed on hematite in this experiment is what indirectly allows us to determine information about the doping particles (thulium oxide). As the sample is mechanochemically activated, the parameters change creating subspectra which reveal information about the behavior of thulium as it gradually substitutes in for iron.

Figure 4(a–e) and (f–j) shows the room-temperature transmission Mössbauer spectra of the xTm_2O_3-$(1-x)\alpha$-Fe_2O_3 series at milling times of 0-12 hours for molar concentrations x=0.1 and 0.5, respectively. The spectra corresponding to 0 hours of milling time were fitted with a sextet with the hyperfine magnetic field of 51.9 T, representing hematite. A small quadrupole-split doublet was added to these fits to account for the presence of ultrafine hematite nanoparticles, with the dimension less than 7 nm.

A second six-line pattern was introduced in the analysis of the Mössbauer spectra in Figure 4 (b–e) and (g–j), with the magnetic hyperfine field around 47 T (smaller than that of hematite) and assigned to thulium-doped hematite nanoparticles, $Tm:Fe_2O_3$. This sextet originates from substitutions of Fe atoms by nonmagnetic Tm atoms and is consistent with the model of local atomic environment. In addition, a third sextet, with a BHF of about 35 T, was necessary in the Mössbauer spectra of Figure 4(c–e) and (i–j), demonstrating an increased level of Tm substitutions in the system subjected to milling.
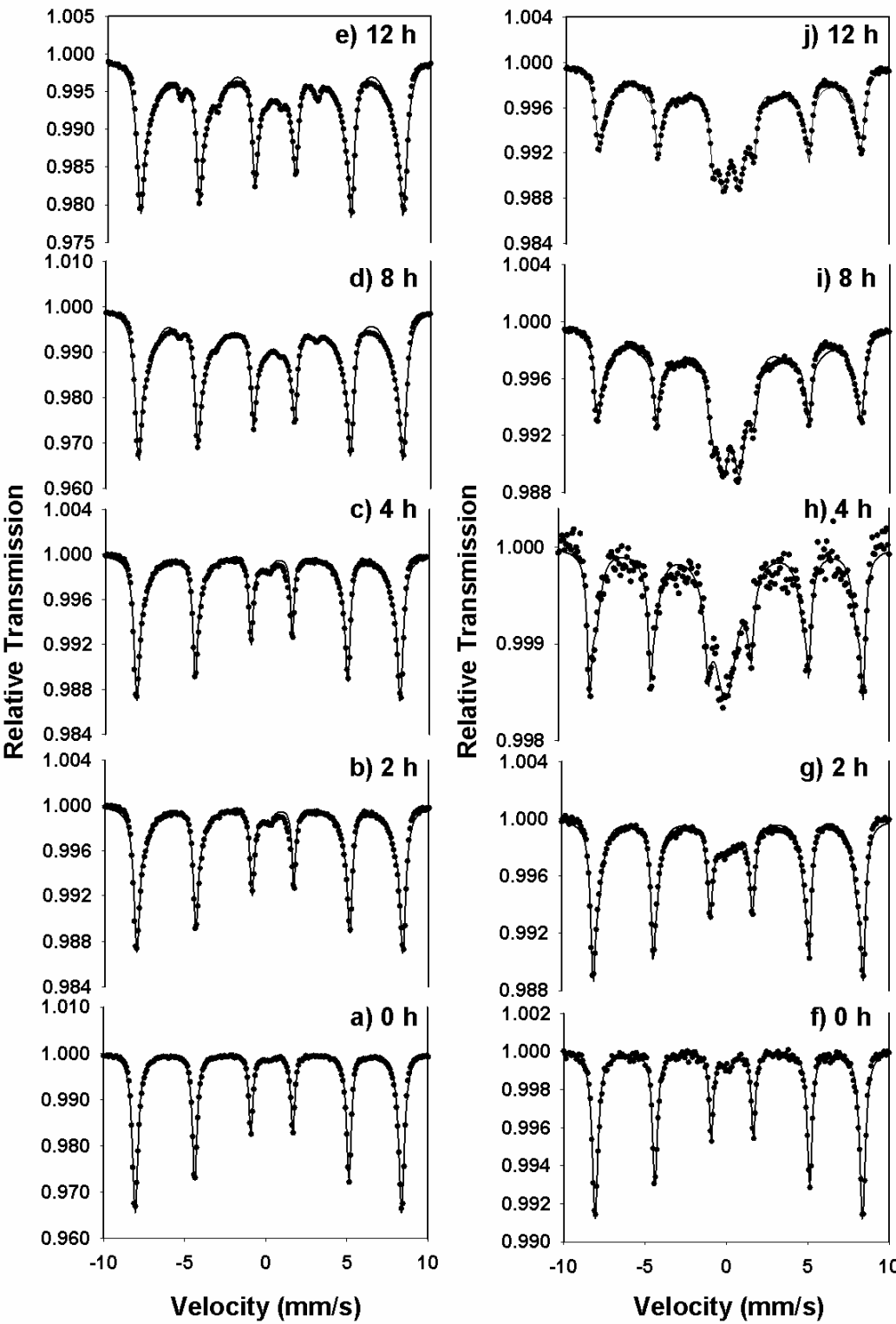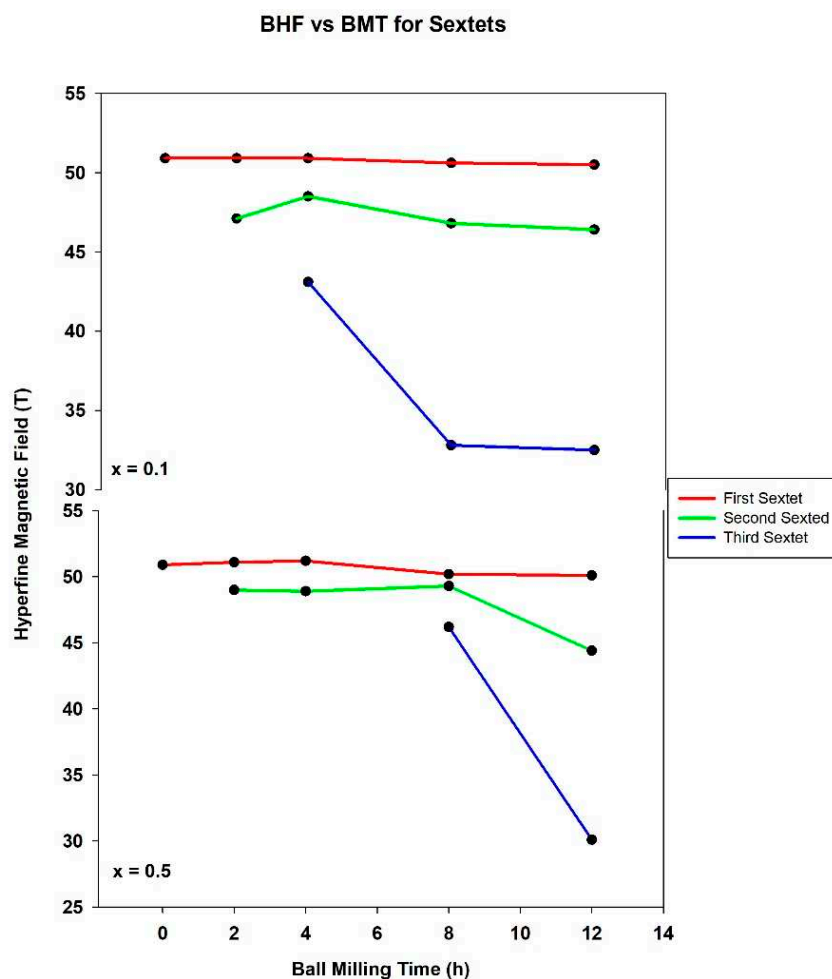
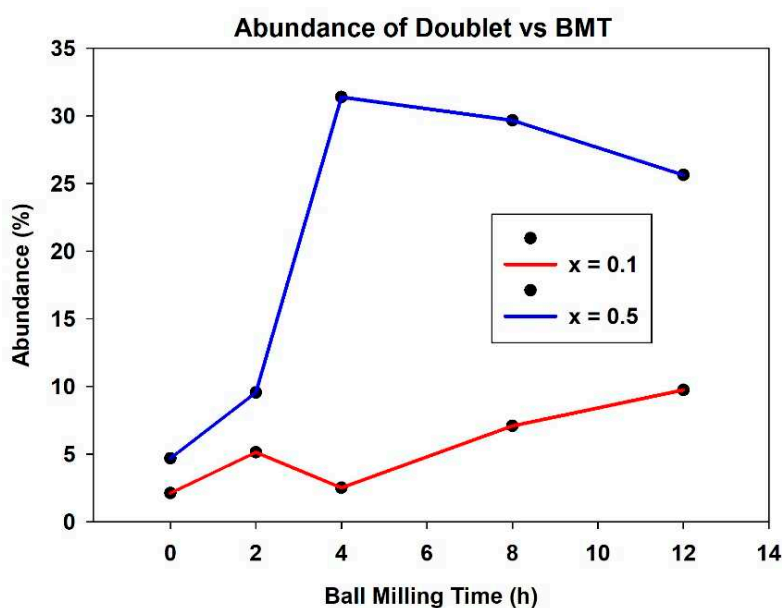**Figure 4.** Mössbauer spectra for x=0.1 (**a-e**) and x=0.5 (**f-j**).

Figure 5. Magnetic hyperfine fields as function of ball milling time for the three sextets involved at both molar concentrations.

The dependence of the BHF values of these sextets on the ball milling time is depicted in Figure 5 and indicates the formation of a limited solid solution in the studied samples. A higher level of substitution is not possible due to the difference in the ionic radii of the Tm^{3+} ions (1.02 Å) and Fe^{3+} ions (0.645 Å). It may be noted that the formation of a solid solution was also observed for the system xGd_2O_3-$(1-x)\alpha$-Fe_2O_3 [15], but was not observed in the xNd_2O_3-$(1-x)\alpha$-Fe_2O_3 system reported previously, due to the specific chemistry of the Nd ions [16].

In addition to the three sextets, a quadrupole-split doublet was introduced in the fitting of milled specimens, with a quadrupole splitting QS of ~0.25 mm/s and isomer shift IS of ~0.1 mm/s. As can be seen in Figure 6, its abundance as function of BMT increases up to 10% of the total spectral area for x=0.1 and to about 30% for the x=0.5 substitution level. The doublet can be assigned to the formation of thulium iron perovskite (thulium orthoferrite), which is believed to be governed by the reaction $Tm_2O_3 + Fe_2O_3 \rightarrow 2TmFeO_3$, which occurs during the mechanochemical activation process [17]. The precipitation of thulium orthoferrite is more pronounced at the greater molarity employed and essentially increases as function of the ball milling time for both molar concentrations.

Abundance of Doublet vs BMT

Figure showing Abundance (%) vs Ball Milling Time (h) with two curves: x = 0.1 (red) and x = 0.5 (blue).

Figure 6. Abundance of the quadrupole doublet as function of ball milling time for both molar concentrations.

It can be seen in Figure 6 that there is certainly a positive relationship between mechanochemical activation and increase in doublet occupation of the spectral graph. The initial increase in the doublets from samples with no ball milling time to the higher ball milling time samples is due to the appearance of thulium iron perovskite in addition to the superparamagnetic particles which were the only cause of the doublets in zero ball milling time samples. For the higher concentration samples, there was a dramatic increase in the abundance of the doublet from 2 ball milling hours to 4. This is evident on the spectral graphs where the central peaks suddenly elongate and the quadrupole splitting of the doublet becomes evident upon initial observation. The x=0.5 samples with ball milling times above this (8 hours and 12 hours) retain the same, highly abundant quadrupole split doublets. Samples with the same concentration but less ball milling time, as well as all x=0.1 concentration samples have a much smaller abundance of doublets (also evident upon observation of the spectral graphs). This is in keeping with theory, as the samples with lower concentration have less Tm ion substitution into the lattice, so there is less reduction of the magnetic hyperfine field to create these dramatic doublets. The doublets are caused by the precipitation of the thulium iron perovskite phase during mechanochemical activation. Similarly, samples with less ball milling time have less swapping of ions because they have less mechanochemical activation which allows for this substitution. Looking at Figure 6 generally, one can see that the quadrupole split doublet increases in abundance from 5.14 and 9.56% at 2 hours ball milling time (x=0.1 and x=0.5, respectively) to 9.75 and 25.64% at 12 hours ball milling time.

Perhaps the most obvious manifestation of the thulium substitution into the hematite lattice is the changing of hyperfine magnetic field values for separate sextets of each spectrum. Figure 5 plots these values as a function of ball milling time. The first sextet for each spectrum (represented in red) displays a relatively flat trend across the graph. The interpretation of this being that the first sextet represents the remaining hematite lattice points where the Fe^{3+} ions have little to no neighboring Tm^{3+} ions, resulting in a sextet with a hyperfine magnetic field at the accepted value of 51.9 T. Below this is another relatively flat line for the hyperfine magnetic field of the second sextet. For both concentrations, the parameter remained between 44 T and 50 T. This is in keeping with theory as after 2 hours of ball milling the substitution of thulium into the lattice should create a sextet with a reduced field. In other words, this sextet represents the spectroscopic results for iron ions with more neighboring thulium ions in the lattice than the first sextet in that sample. In each concentration the third sextet shows a large drop in magnetic field from around 45 T to closer to 30 T. Though this measurement does not appear as fixed as those of the previous two sextets, fit is also in good keeping

with theory. The longer the sample is ball milled, the more the overall magnetic field should be lowered, which is still the case. The contrast in measurements is likely due to a dramatic increase in thulium substitution into the lattice. Afterall, the longer the sample is milled, the higher the likelihood becomes that a substitution will occur.

3. Materials and Methods

In order to determine magnetic and chemical information about thulium oxide (Tm_2O_3), samples of thulium oxide and hematite were ground in air and combined (in different concentrations) to obtain a mixed oxide sample of the type $xTm_2O_3*(1-x)\alpha\text{-}Fe_2O_3$. The two different prepared concentrations of thulium oxide-hematite were x=0.1 and x=0.5. The precursor powders of hematite and thulium oxide with particle sizes of 50 and 90 nm, respectively were purchased from Alfa Aesar. Five samples in each concentration were prepared. Samples were then mixed manually using a mortar and pestle and introduced into a hardened steel vial along with twelve stainless steel balls. These vials were loaded into a Spex 8000 mixer mill, which has the capability to grind or mill (high energy ball mill or shaker mill) samples. This model has a speed of 1060 cycles per minute. The samples were then milled for a variation of hours ranging from 0 hours to 12 hours such that one of each concentration was milled for 0 hours, 2 hours, 4 hours, 8 hours and 12 hours. High energy ball milling is known to make samples amorphous and to nanocrystallize them. In other studies, ball milling of thulium oxide was found to completely turn into its amorphized state and the thulium and oxygen particles dissolved into the lattice of the material which they were milled with. After 48 hours of milling, they created a fully mixed solid solution [2].

After its ball milling time, each sample was analyzed in a constant acceleration spectrometer SeeCo device with a 25 mCi [57]Co gamma ray source diffused in a Rh matrix. At a constant acceleration, this source emitted gamma rays which were absorbed by the post ball milled samples of thulium oxide-hematite. The samples were analyzed at room temperature. The resulting spectra were recorded and analyzed by least-squares fitting with the WinNORMOS program in the assumption of Lorentzian lineshapes. The graphs on WinNORMOS plot the intensity of the spectra in counts or the relative transmission on the vertical axis and relative velocity between source and absorber on the horizontal axis. Isomer shifts of the recorded spectra are relative to the gamma ray source of the spectrometer.

4. Conclusions

Two different concentrations (x=0.1 molarity and x=0.5 molarity) of thulium oxide in hematite were synthesized using high energy ball milling. The mechanochemically activated samples were analyzed using Mössbauer spectroscopy with a Co^{57} gamma ray source. The results of the spectroscopy were reviewed using the WinNORMOS software package which uses the least squares fitting method of the Lorentzian line shapes of the data. It was found that as the ball milling time increased, so did the relative abundance of the quadrupole split doublet on the spectral graphs. The initial doublet for samples with zero ball milling time is due to the presence of superparamagnetic hematite particles in the sample. The increase in quadrupole split doublet abundance after ball milling is indicative of the formation of a thulium oxide perovskite phase as a byproduct of the mechanochemical activation of the sample. Also, the results of this experiment show that as the ball milling time increases, new sextets are formed which have a lower hyperfine magnetic field than the initial sextet (representative of hematite at 51.9 T). This supports the supposition that the high energy ball milling of the samples causes a point defect in the hematite lattice. This defect is the substitution of thulium where iron was previously positioned in the lattice, subsequently lowering the hyperfine magnetic field of the solid. The phase outcome consisted of a solid solution of thulium-doped hematite and the formation of thulium orthoferrite. The fundamental microscopic mechanism explaining the phase sequence is related to the mutual substitutions of Tm ions in the hematite lattice and Fe ions in the thulium oxide lattice.

This study also opens the door for many other experiments which might add to the knowledge of the physical properties of thulium oxide. In addition to the Mössbauer spectra, low

temperature spectroscopy may be performed to observe the behavior of the substance at temperatures around 5 K. Differential scanning calorimetry may be used to examine the thermal stability, heat capacity or other thermal properties of thulium oxide through the examination of the heat flow of the sample as a function of temperature. The thermal decomposition, phase transitions or oxidation of thulium oxide could be explored with the use of thermal gravimetric analysis which measures sample mass as heat is gradually added. Also, the crystal structure of thulium oxide could be more thoroughly understood with the performance of x-ray diffraction.

There are already various uses for rare earth metal oxides, thulium oxide and hematite in particular [24–30]. This study scratches the surface of the physical details of the compound. Through implementation of other methods which would examine many more properties of thulium oxide than what was discussed here, we may not only better understand the current usefulness of the solid but even discover other to make use of it.

Conflicts of Interests: There are no conflicts of interests with this paper.

References

1. Luo, Y.; Ran, G.; Chen, N.; Wang, C., Microstructure and morphology of Mo-based Tm_2O_3 composites synthesized by ball milling and sintering, *Advanced Powder Technology* **(2017)** *28*, 658-664.
2. Mu, Y.; Ran, G.; Wu, W.; Ye, C., Ball milling properties and sintering behavior of Fe- Tm_2O_3 mixture powders, *Advanced Powder Technology* **(2019)** *30*, 2548-2554.
3. Sidorowicz, A.; Wajler, A.; Weglarz, H.; Olszyna, A., Preparation of Tm_2O_3 nanopowders for application in reactive sintering of Tm:YAG, *Ceramics International* **(2014)** *40*, 10269-10274.
4. Sidorowicz, A.; Nakielska, M.; Wajler, A.; Weglarz, H.; Olszyna, A., Effect of Tm_2O_3 doping on microstructure and optical properties of Tm:YAG ceramics, *Ceramics International* **(2015)** *41*, 9051-9056.
5. Xu, X.; Zhu, L.L.; Dai, M.M.; Zhao, C.C.; Zhang, G.X.; Jiang, Y.J.; Lin, H.T., Fabrication and characterization of highly transparent ZrO_2-doped Tm_2O_3 ceramics, *Ceramics International* **(2021)** *47*, 28859-28865.
6. Patil, A.S.; Patil, A.V.; Dighavkar, C.G.; Adole, V.A.; Tupe, U.J., Synthesis techniques and applications of rare earth metal oxides semiconductors: A review, *Chemical Physics Letters* **(2022)** *796*, 139555.
7. Panahi, A.; Monsef, R.; Imran, M.K.; Mahdi, A.A.; Ruhaima, A.A.K.; Salavati-Niasari, M., $TmVO_4/Fe_2O_3$ nanocomposites: Sonochemical synthesis, characterization, and investigation of photocatalytic activity, *International Journal of Hydrogen Energy* **(2023)** *48*, 3916-3930.
8. Singh, J.; Srivastava, M.; Roychoudhury, A.; Lee, D.W.; Lee, S.H.; Malhotra, B.D., Optical and electro-catalytic studies of nanostructured thulium oxide for vitamin C detection, *Journal of Alloys and Compounds* **(2013)** *578*, 405-412.
9. Yu, H.B.; Yu, P.; Bai, H.Y., Lutetium and thulium based rare earth bulk metallic glasses, *Journal of Non-Crystalline Solids* **(2008)** *354*, 4539-4542.
10. Zeng, X.; Fu, X.; Xi, X.; Wang, D.; Zhou, J.; Li, B., Thermodynamics of spin reorientations in $TmFeO_3$ ceramics observed with terahertz time domain spectroscopy, *Materials Letters* **(2016)** *164*, 64-67.
11. Mitrovic, I.Z.; Althobaiti, M.; Weerakkody, A.D.; Sedghi, N.; Hall, S.; Dhanak, V.R.; Chalker, P.R.; Henkel, C.; Dentoni Litta, E.; Hellstrom, P.E.; Ostling, M., Interface Engineering of Ge using thulium oxide: Band line-up study, *Microelectronic Engineering* **(2013)** *109*, 204-207.
12. Adzimnuddin, M.; Latiff, A.A.; Hazura, H.; Ahmad, M.T.; Harun, S.W., Thulium oxide film as a passive saturated absorber for pulsed fiber laser generation, *Optical Fiber Technology* **(2020)** *58*, 102249.
13. Deng, J.; Quah, H.J., Structural, morphological and metal-oxide-semiconductor characteristics of thulium oxide passivation layer grown in nitrogen-oxygen-nitrogen ambient, *Sustainable Materials and Technologies* **(2023)** *35*, e00534.
14. Meeuwissen, A.; Bosco, G.B.F.; van der Kolk, W., Optical and structural characterization of Tm_2O_3, TmN and TmO_xN_y thin films grown by direct-current reactive magnetron sputtering, *Thin Solid Films* **(2021)** *717*, 138450.
15. Glasser, S.; Craig, A.J.; Tolea, F.; Sofronie, M.; Aitken, J.A.; Sorescu, M., Synthesis and characterization of gadolinium oxide-hematite magnetic ceramic nanostructures, *Journal of Minerals and Materials Characterization and Engineering* **(2023)** *11*, 1-15.
16. Sorescu, M.; Diamandescu, L.; Sofronie, M.; Pratt, C.; Jubeck, J., Mechanochemical synthesis and Mössbauer characterization of neodymium oxide-hematite magnetic ceramic nanoparticles: Phase sequence and recoilless fraction, *Materials Chemistry and Physics* **(2022)** *277*, 125511.

17. Sorescu, M., *Recent Applications of the Mössbauer Effect,* Dorrance Publishing Company, Pittsburgh, USA (2020).

18. Castrillejo, Y.; Fernández, P.; Bermejo, M. R.; Barrado, E.; Martínez, A. M., Electrochemistry of thulium on inert electrodes and electrochemical formation of a Tm-Al alloy from molten chlorides, *Electrochimica Acta* **(2009)** *54*, 6212-6222.

19. Lee, S. W.; Park, S. K.; Min, B.; Kang, J.; Sohn, Y., Structural/spectroscopic analyses and $H_2/O_2/CO$ responses of thulium(III) oxide nanosquare sheets, *Applied Surface Science* **(2014)** *307*, 736-743.

20. Bartl, A.; Dunsch, L.; Kirbach, U., Preparation, mass spectrometry and solid state ESR spectroscopy of endohedral fullerenes, *Solid State Communications* **(1995)** *94*, 827-831.

21. Harker, S. J.; Stewart, G. A.; Edge, A. V. J., Induced thulium magnetization for the *Immm* Phase of Tm_2BaNiO_5, *Solid State Communications* **(1996)** *100*, 307-310.

22. Stewart, G. A.; Gubbens, P. C. M., Induced thulium magnetization in the 'green phase' Tm_2BaCuO_5, *Journal of Magnetism and Magnetic Materials* **(1999)** *206*, 17-26.

23. Limongelli, J.; Tolea, F.; Valeanu, M.; Diamandescu, L.; Xu, T.; Sorescu, M., Nanostructured iridium oxide-hematite magnetic ceramic semiconductors, *Ceramics International* **(2015)** *41*, 333-343.

24. Tadic, M.; Kusigerski, V.; Markovic, D.; Milosevic, I.; Spasojevic, V., Anomalous behavior of the magnetic hysteresis loop in the α-Fe_2O_3/SiO_2 nanocomposite, *Materials Letters* **(2009)** *63*, 1054-1056.

25. Tadic, M.; Panjan, M.; Damjanovic, V.; Milosevic, I., Magnetic properties of hematite α-Fe_2O_3 nanoparticles prepared by hydrothermal synthesis method, *Applied Surface Science* **(2014)** *320*, 183-187.

26. Tadic, M.; Kopanja, L.; Panjan, M.; Kralj, S.; Nikodinovic-Runic, J.; Stojanovic, Z., Synthesis of core-shell hematite (α-Fe_2O_3) nanoplates: Quantitative analysis of the particle structure and shape, high coercivity and low cytotoxicity, *Applied Surface Science* **(2017)** *403*, 628-634.

27. Khani, O.; Shoushtari, M.Z.; Jazirehpour, M.; Shams, M.H., Effect of carbon shell thickness on the microwave absorption of magnetite-carbon core-shell nanoparticles, *Ceramics International* **(2016)** *42*, 14548-14556.

28. Woo, K.; Lee, H.J., Synthesis and magnetism of hematite and maghemite nanoparticles, *Journal of Magnetism and Magnetic Materials* **(2004)** *272-276*, e1155-e1156.

29. Tadic, M.; Kusigerski, V.; Markovic, D.; Milosevic, I.; Spasojevic, V., High concentration of hematite nanoparticles in a silica matrix: Structural and magnetic properties, *Journal of Magnetism and Magnetic Materials* **(2009)** *321*, 12-16.

30. Jacob, J.; Khadar, M.A., VSM and Mossbauer study of nanostructured hematite, *Journal of Magnetism and Magnetic Materials* **(2010)** *322,* 614-621.